Available online at www.sciencedirect.com
SCIENCE DIRECT
Journal of Organometallic Chemistry 691 (2006) 3298–3304
Journal of Organometallic Chemistry
www.elsevier.com/locate/jorganchem

The photochemistry of (η^3-2-R-C_3H_4)Fe(CO)(NO)(X) (R = H or Cl; X = CO or PPh_3) in room temperature solution or frozen gas matrixes

Conor Long *, Kieran Maher, Mary T. Pryce

School of Chemical Sciences, Dublin City University, Dublin 9, Ireland

Received 26 January 2006; received in revised form 6 April 2006; accepted 11 April 2006
Available online 21 April 2006

Abstract

A photochemical study of allyl iron complexes of the type, (η^3-2-R-C_3H_4)Fe(CO)(NO)(X) (R = H or Cl; X = CO or PPh_3) is presented. These compounds were studied in solid matrixes at 20 K, and at room temperature, by a combination of laser flash at 355 nm and steady-state photolysis. The predominant photochemical process for these compounds is loss of a CO ligand. In addition, exhaustive irradiation of (η^3-2-R-C_3H_4)Fe(CO)(NO)(PPh_3) with $\lambda_{exc} > 300$ nm provided evidence for a haptotropic shift of the allyl group from η^3 to η^1 coordination.

Keywords: Iron; Carbonyl; Nitric oxide; Flash photolysis; Photochemistry; Matrix isolation

1. Introduction

The importance of nitric oxide in biological functions has stimulated much interest in recent years in the chemistry and biochemistry of nitrosyl complexes. The biological roles of nitric oxide have been summarised as regulatory (e.g. immune or neurotransmission), protective (e.g. free radical scavenging or antitumour activity) and deleterious (e.g. enzyme inhibition or myocardial stunning) [1]. As the various roles of NO have only recently been understood, it is not surprising that metalonitrosyl complexes have become an active area of research due to their potential as a controlled means of releasing NO in biological systems [2].

Nitric oxide is a 15 electron stable radical, a feature which dominates its physiological roles. As the molecule controls the activity of different enzymes via coordination to heme and non-heme centres, interest has centred on iron nitrosyl complexes.

Photochemical studies on simple organometallic systems have demonstrated that NO release can be achieved under photochemical conditions [3,4]. Low temperature photolysis of $Fe(CO)_5$ in NO doped matrixes results in the formation of $Fe(CO)_2(NO)_2$, which subsequently looses NO to regenerate the starting material $Fe(CO)_5$ [3]. This matrix isolation study at 20 K, also reported the photochemical loss of NO from $Co(CO)_3NO$ and $Mn(CO)_4NO$ [3]. Time-resolved infrared studies at 355 nm excitation of $Co(CO)_3NO$ in the gas phase resulted in both NO and CO elimination, giving rise to both $Co(CO)_3$ and $Co(CO)_2NO$, with scission of the Co–NO bond favoured.

Flash photolysis studies of various NO-bound iron porphyrins and heme proteins, have shown that these complexes undergo NO labilisation [5]. The photochemistry of Roussin's black salt, $[Fe_4S_3(NO)]^{7-}$, Roussin's red salt, $[Fe_2S_2(NO)_4]^{2-}$, and the red salt esters $[Fe_2(SR)_2(NO)_4]$ have been studied by Ford and co-workers as precursors for biological nitric oxide delivery [6,7]. A combination

* Corresponding author. Tel.: +353 1 7008001; fax: +353 1 7005503.
E-mail address: conor.long@dcu.ie (C. Long).

0022-328X/$ - see front matter © 2006 Elsevier B.V. All rights reserved.
doi:10.1016/j.jorganchem.2006.04.004

of flash photolysis studies and continuous photolysis confirmed NO cleavage in these systems. The second order rate constant for the reaction of $[Fe_2S_2(NO)_3]^{2-}$ with NO was reported to be 9×10^8 M^{-1} s^{-1}.

In this paper we report the results of a series of photochemical investigations on (η^3-C_3H_4R)Fe(CO)(X) NO complexes (R = H or Cl; X = CO or PPh_3). We have investigated the photochemistry of these complexes using a combination of flash photolysis with UV–Vis monitoring and steady-state photolysis experiments in order to investigate these compounds as potential sources of photogenerated NO.

2. Results and discussion

The spectroscopic parameters for the compounds under investigation are presented in Table 1 and the UV–Vis and IR spectra of (η^3-C_3H_5)$Fe(CO)_2(NO)$ in cyclohexane are given in Figs. 1 and 2, respectively. The equivalent IR band positions for (η^3-2-Cl-C_3H_4)$Fe(CO)_2(NO)$ are shifted to higher energy (Table 1) compared to those for (η^3-C_3H_5)$Fe(CO)_2(NO)$ because of the electron withdrawing effect of chlorine. The absorption shoulder at 380 nm in the UV–Vis spectrum of the chloro-compound is less pronounced than that observed for (η^3-C_3H_5)$Fe(CO)_2(NO)$. As the absorption of both compounds extends well into the visible region of the spectrum, initial photochemical experiments used excitation wavelengths ($\lambda_{exc} > 500$ nm). However, no photochemical changes were observed in these experiments.

2.1. The steady-state photolysis of (η^3-2-R-C_3H_4)$Fe(CO)_2(NO)$ in room temperature cyclohexane in the presence of PPh_3 (R = H or Cl)

Photolysis of (η^3-2-R-C_3H_4)$Fe(CO)_2(NO)$ with $\lambda_{exc} >$ 340 nm in degassed cyclohexane in the presence of a 10-fold excess of PPh_3, resulted in a reduction in the intensity of the bands of (η^3-2-R-C_3H_4)$Fe(CO)_2(NO)$ in the IR spectrum and the production of bands that can be assigned to the appropriate (η^3-2-R-C_3H_4)Fe(CO)(NO)(PPh_3) compound (see Fig. 3 and Table 1). The general shift to lower energy of the ν_{CO} and ν_{NO} bands reflects the greater electron density on the iron atom when the PPh_3 ligand is present compared to a CO ligand. These experiments clearly indicate that CO-loss is the dominant photochemical reaction for this class of compound. Similar experiments using UV–Vis spectroscopy showed only a general increase in

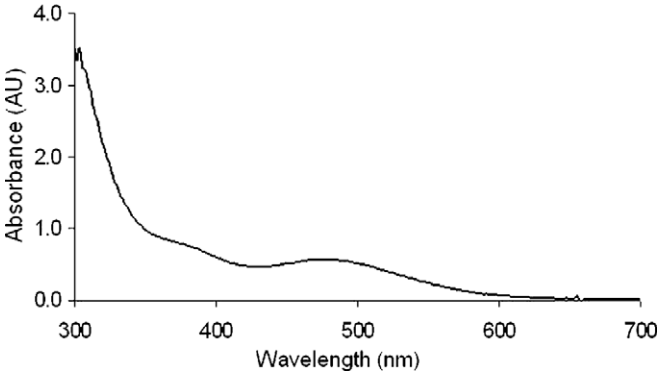

Fig. 1. The UV–Vis spectrum of (η^3-C_3H_5)$Fe(CO)_2(NO)$ in cyclohexane (2.2×10^{-3} M) showing an absorption shoulder at 380 nm and a broad maximum at 480 nm.

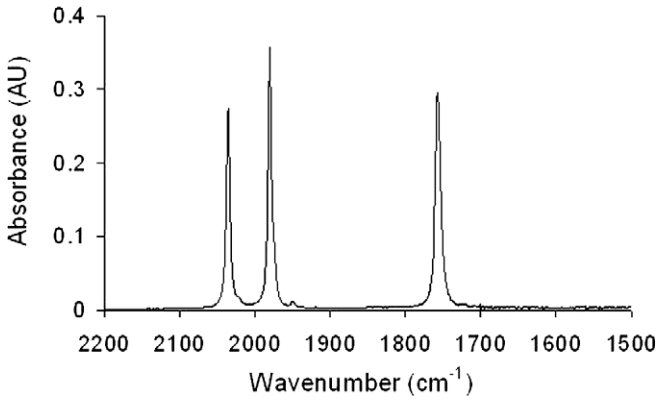

Fig. 2. The IR spectrum of (η^3-C_3H_5)$Fe(CO)_2(NO)$ in cyclohexane solution (arbitrary concentration) in the ν_{CO} and ν_{NO} region.

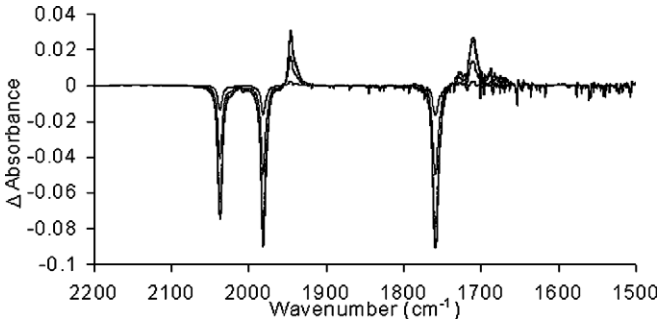

Fig. 3. An IR difference spectrum obtained following photolysis of (η^3-C_3H_5)$Fe(CO)_2(NO)$ in cyclohexane solution in the presence of a 10-fold excess of PPh_3 using $\lambda_{exc} > 340$ nm at room temperature. The ν_{NO} bands are close to the region where atmospheric water vapour absorbs, hence the high level of noise in this region.

Table 1
Principal spectroscopic features of the compounds in this investigation

Compound	λ_{max} (nm)	ν_{CO} (cm^{-1})	ν_{NO} (cm^{-1})
(η^3-C_3H_5)$Fe(CO)_2(NO)$	480	2036, 1980	1757
(η^3-2-Cl-C_3H_5)$Fe(CO)_2(NO)$	480	2045, 1993	1759
(η^3-C_3H_5)Fe(CO)(NO)(PPh_3)	380	1945	1709
(η^3-2-Cl-C_3H_5)Fe(CO)(NO)(PPh_3)	380	1949	1713

absorption across the entire spectrum which points to the formation of a precipitate during photolysis. As these results demonstrated that CO-loss could be achieved under photochemical conditions, monochromatic light sources were used to further probe the photochemistry of these compounds.

2.2. Laser flash photolysis of (η^3-2-R-C_3H_4)Fe(CO)$_2$(NO) (R = H or Cl; λ_{exc} = 355 nm) in cyclohexane in the presence of CO

Flash photolysis of (η^3-2-R-C_3H_4)Fe(CO)$_2$(NO) produced a broad featureless transient absorption spectrum. Fig. 4 contains a typical transient signal obtained following photolysis of (η^3-C_3H_5)Fe(CO)$_2$(NO) in CO saturated cyclohexane (S) solution. The transient absorption signal decayed within 100 μs to its pre-irradiation value, indicating that under these conditions there is a full recovery of the parent complex concentration following photolysis. The lifetime of the transient species was dependent on the concentration of CO. This behaviour is typical of CO-loss intermediates [8]. Consequently we have assigned this transient absorption to the appropriate CO-loss intermediate as outlined in Reaction (1) (S = solvent). The second order rate constants for these reactions are presented in Table 2. On changing the substituent on the allyl ligand from H to Cl little variation in the second order rate constant was observed ($4.4\ (\pm 0.5) \times 10^6\ M^{-1}\ s^{-1}$ for (η^3-C_3H_5)Fe(CO)$_2$(NO) and $6.8\ (\pm 0.5) \times 10^6\ M^{-1}\ s^{-1}$ for (η^3-2-Cl-C_3H_4)Fe(CO)$_2$(NO)). During the course of these experiments, the steady-state UV–Vis spectrum of the solution was monitored, and this showed negligible changes, confirming that the overall photochemical process was reversible.

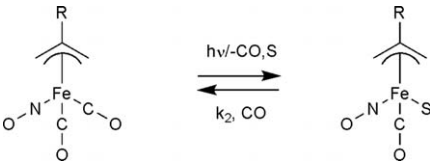

(1)

2.3. Laser flash photolysis of (η^3-2-R-C_3H_4)Fe(CO)$_2$(NO) (R = H or Cl; λ_{exc} = 355 nm) under an argon atmosphere

Pulsed photolysis of (η^3-2-R-C_3H_4)Fe(CO)$_2$(NO) in degassed cyclohexane under an argon atmosphere produced a broad featureless transient absorption spectrum. A typical transient signal observed at 360 nm is presented in Fig. 5 for R = H. This signal exhibits a significant residual absorption indicating the formation of a photoproduct, which is stable on the time-scale of the experiment. The steady-state UV–Vis spectrum of the solution was monitored throughout these experiments and exhibited a general increase in absorbance across the entire spectrum, being most pronounced in the 340–500 nm region. In addition an IR spectrum of the solution obtained immediately after the flash photolysis experiments revealed two new features in the ν_{CO} and ν_{NO} region at 1965 and 1703 cm^{-1} (Fig. 6). The formation of dinuclear species by the reaction of CO-loss intermediates with the parent compound is frequently observed following flash photolysis of metal carbonyl compounds in the absence of trapping ligands such as CO [9]. The formation of a dinuclear species could be responsible for the additional features observed in the IR spectrum reported here. It is clear, however, that this species is not stable in the long term, and reacts with the photoproduced CO, reforming the parent compound.

2.4. Matrix isolation studies of (η^3-allyl)Fe(CO)$_2$NO in an argon matrix at 20 K

Matrix isolation studies with IR monitoring in an argon matrix were carried out at 20 K. As (η^3-allyl)Fe(CO)$_2$NO

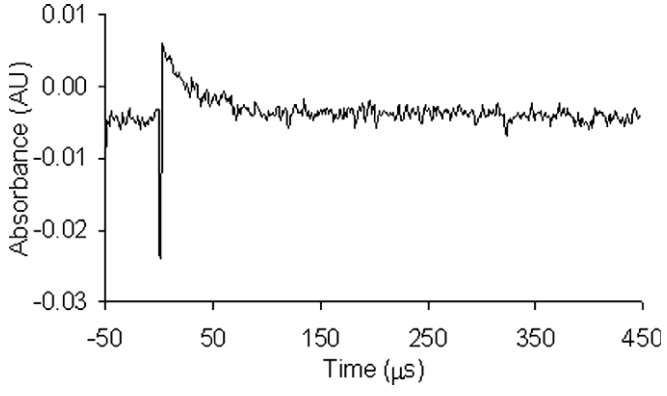

Fig. 4. A typical transient signal obtained following the flash photolysis of (η^3-C_3H_5)Fe(CO)$_2$(NO) in cyclohexane in the presence of CO ([CO] = 1.1×10^{-2} M).

Table 2
The second order rate constants (k_2) for Reaction (1) at 298 K

R	k_2[a] ($M^{-1}\ s^{-1}$)
H	4.4×10^6
Cl	6.8×10^6

[a] Estimated errors on these measurements ±10%.

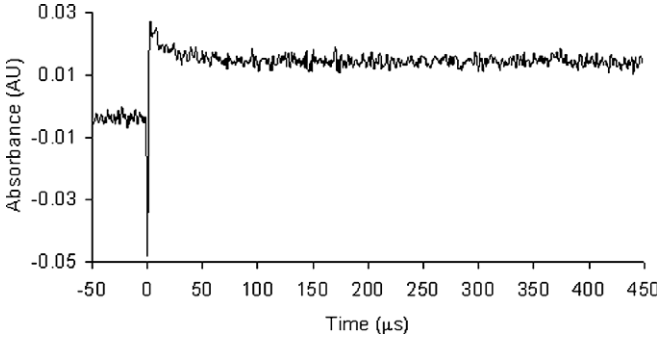

Fig. 5. Transient signal observed at 360 nm following flash photolysis of (η^3-C_3H_5)Fe(CO)$_2$(NO) in cyclohexane under an argon atmosphere (λ_{exc} = 355 nm) showing the formation of a long-lived species.

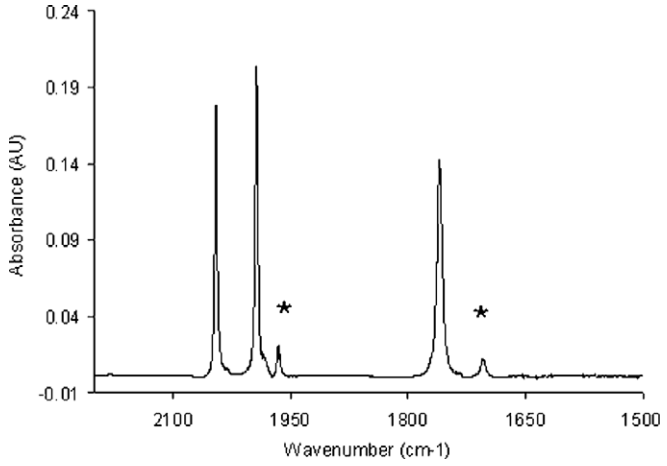

Fig. 6. The infrared spectrum obtained immediately following flash photolysis of $(\eta^3\text{-}2\text{-}Cl\text{-}C_3H_4)Fe(CO)_2(NO)$ in cyclohexane solution under an argon atmosphere, showing additional features (★) at 1965 and 1703 cm^{-1} to those of the parent compound at 2045, 1993, and 1760 cm^{-1}. These additional features had disappeared when the spectrum of the same solution was measured 12 h later.

has characteristic ν_{CO} and ν_{NO} signatures in the IR, any changes in electron density at the metal centre should be observed. The ν_{CO} absorptions for $(\eta^3\text{-allyl})Fe(CO)_2NO$ occur at 2040 and 1985 cm^{-1} with the ν_{NO} absorption at 1764 cm^{-1} in an Ar matrix. Initial photolysis of the sample ($\lambda_{exc} > 500$ nm) led to a small decrease in intensity of ν_{CO} and ν_{NO} of $(\eta^3\text{-allyl})Fe(CO)_2NO$, however, no new bands were formed, indicating decomposition of $(\eta^3\text{-allyl})Fe(CO)_2NO$. Subsequent photolysis ($\lambda_{exc} > 400$ nm) led to a further decrease in absorbance of these bands, with the formation of a weak band at 2139 cm^{-1}, indicating the presence of "free" CO in the matrix. No evidence for either carbonyl or nitrosyl photoproducts were observed at 20 K.

2.5. The steady-state photochemistry of $(\eta^3\text{-}C_3H_5)Fe(CO)(NO)(PPh_3)$

The photochemistry of $(\eta^3\text{-}C_3H_5)Fe(CO)(NO)(PPh_3)$ in cyclohexane solution at room temperature exhibits a wavelength dependence which can be explained in terms of a sequence of photochemical events. For example, broad-band photolysis ($\lambda_{exc} > 410$ nm) of $(\eta^3\text{-}C_3H_5)Fe(CO)(NO)(PPh_3)$ in degassed cyclohexane in the presence of a 10-fold excess of PPh_3 in a sealed cell, produced the IR spectral changes presented in Fig. 7(a). These changes are consistent with the photochemical loss of CO to produce $(\eta^3\text{-}C_3H_5)Fe(NO)(PPh_3)_2$, which exhibits a ν_{NO} band at 1667 cm^{-1} (Scheme 1). However, using shorter wavelength excitation ($\lambda_{exc} > 300$ nm) results in more complicated spectral changes as outlined in Fig. 7(b). Initially (15 min irradiation) the bands of the parent compound $(\eta^3\text{-}C_3H_5)Fe(CO)(NO)(PPh_3)$ were diminished and the ν_{NO} band of $(\eta^3\text{-}C_3H_5)Fe(NO)(PPh_3)_2$ was produced. Further photolysis (total 30 min) produced weak features at 2034, 1978, and 1756 cm^{-1} indicating the formation of $(\eta^3\text{-}C_3H_5)Fe(CO)_2(NO)$ produced by photochemical loss of PPh_3 from $(\eta^3\text{-}C_3H_5)Fe(CO)(NO)(PPh_3)$ followed by reaction with residual CO (Scheme 2). Prolonged (total 60 min) photolysis produced a further two bands at 1890 and 1683 cm^{-1} (this lower energy band overlaps the ν_{NO} band of $(\eta^3\text{-}C_3H_5)Fe(CO)(NO)(PPh_3)$). These bands have been assigned to the haptotropic shift product $(\eta^1\text{-}C_3H_5)Fe(CO)(NO)(PPh_3)_2$ (Reaction (2)) [10]. The apparent depletion of the 1587 cm^{-1} band can be explained by the reduction in the concentration of free PPh_3 during these reactions. Finally, a very weak feature at 1814 cm^{-1} was also observed but the identity of this species remains uncertain.

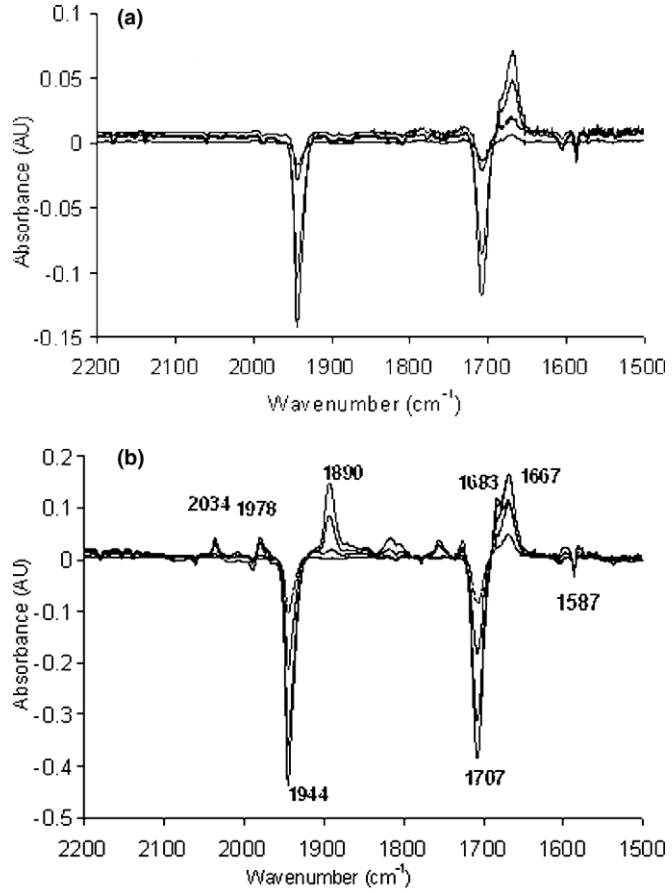

Fig. 7. (a) IR difference spectra obtained following broad-band photolysis ($\lambda_{exc} > 410$ nm) of $(\eta^3\text{-}C_3H_5)Fe(CO)(NO)(PPh_3)$ in degreased cyclohexane in the presence of a 10-fold excess of PPh_3. These spectra show the reduction in band intensity at 1944 and 1707 cm^{-1} which correspond to $(\eta^3\text{-}C_3H_5)Fe(CO)(NO)(PPh_3)$ and the production of a new band at 1667 cm^{-1}, assigned to $(\eta^3\text{-}C_3H_5)Fe(NO)(PPh_3)_2$; (b) IR difference spectra obtained following broad band photolysis ($\lambda_{exc} > 300$ nm) of $(\eta^3\text{-}C_3H_5)Fe(CO)(NO)(PPh_3)$ with excess PPh_3 showing the formation of $(\eta^1\text{-}C_3H_5)Fe(CO)(NO)(PPh_3)_2$ (1890 and 1683 cm^{-1}).

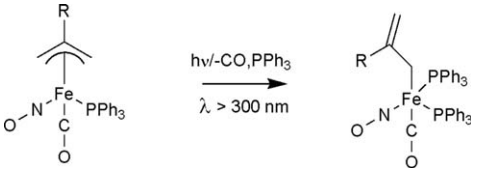

(2)

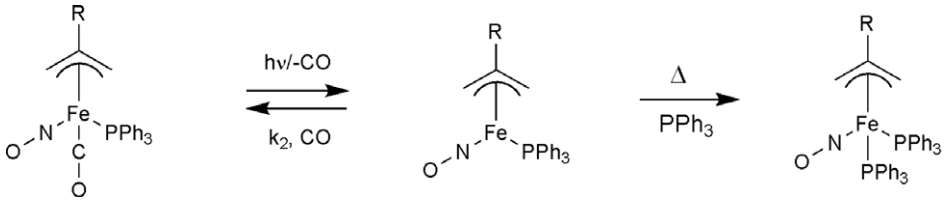

Scheme 1.

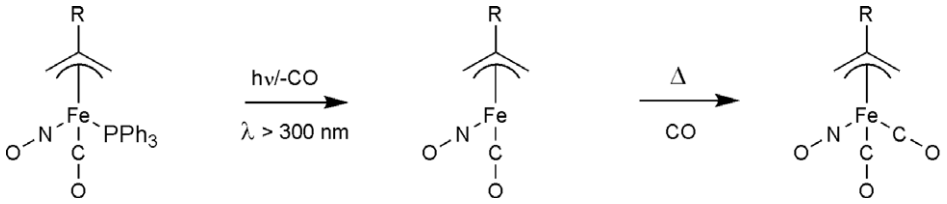

Scheme 2.

2.6. Laser flash photolysis (λ_{exc} = 355 nm) of (η^3-C_3H_5)Fe(CO)(NO)(PPh_3) in toluene solution at room temperature

Because of the low solubility of (η^3-C_3H_5)Fe(CO)-(NO)(PPh_3) in cyclohexane a series of flash photolysis experiments were conducted in toluene solution. The ground-state absorbance spectrum of (η^3-C_3H_5)Fe(CO)-(NO)(PPh_3) in toluene exhibits broad unresolved features at wavelengths less than 600 nm (Fig. 8). The time-resolved signals obtained following pulsed photolysis (λ_{exc} = 355 nm) can be explained by a parent bleach and recovery process (see inset of Fig. 8). The maximum bleach signals were obtained at 420 nm and this wavelength was used to measure its kinetic parameters. The observed rate constant for the recovery in the presence of CO (5×10^{-3} M) was 4.3 (± 0.5) $\times 10^4$ s^{-1} implying a second order rate constant (k_2 at 298 K) of 8.6 (± 0.5) $\times 10^6$ M^{-1} s^{-1} and under these conditions the absorbance fully recovered to the pre-irradiated value (Fig. 8, inset). It would appear from this rate constant that unlike the group 6 systems the coordinatively unsaturated iron compounds do not interact significantly with the solvent molecules [11]. The reversible nature of the system was confirmed by monitoring the steady-state UV–Vis spectrum of the solution throughout the experiment, which showed no changes. However, in the absence of CO a residual absorbance remained following the laser pulse and the steady-state UV–Vis spectrum showed small changes in the 350–400 nm region. These results are consistent with loss of CO as the primary photochemical event following irradiation with 355 nm photons. In the presence of added CO this process is fully reversible, while in the absence of added CO the CO-loss intermediate reacts with the parent (η^3-C_3H_5)Fe(CO)(NO)(PPh_3) to form a long-lived dinuclear species as frequently observed with other systems (Scheme 3) [7].

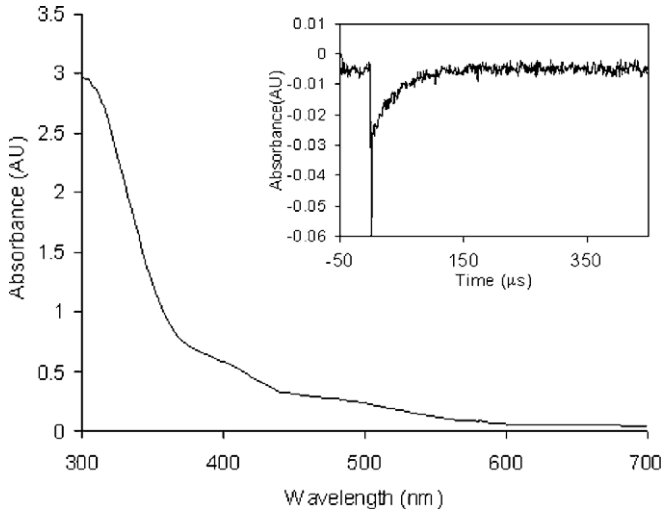

Fig. 8. The UV–Vis spectrum of (η^3-C_3H_5)Fe(CO)(NO)(PPh_3) in toluene solution showing broad unresolved features across the spectrum. The inset shows the bleach and recovery signal at 420 nm obtained following pulsed photolysis (λ_{exc} = 353 nm), in the presence of CO (9×10^{-3} M).

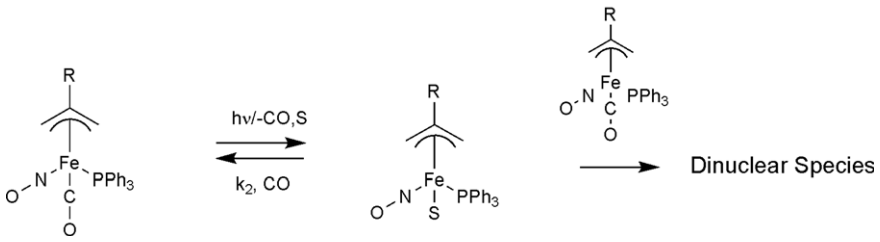

Scheme 3.

3. Summary and conclusion

The time-resolved studies together with the continuous irradiation experiments obtained in this study, confirms loss of CO for all the compounds studied, with no evidence for cleavage of NO. Assignments of the photoproducts were based on the IR experiments, which were carried out in the presence of triphenylphosphine as a trapping ligand. Previously it has been suggested, that NO loss proceeds by an associative mechanism, but no evidence for NO loss was obtained in this study even when the photochemistry was carried out in the presence of a trapping ligand.

4. Experimental

4.1. Reagents

All manipulations were performed under an argon atmosphere. $Fe(CO)_5$, allyl bromide, 2,3-dichloropropene, triphenylphosphine, and bis-diphenylphosphino ethane (all Aldrich Chemical) were used without further purification. Silica gel, (pH 6.5–7.5) was supplied by B. F. Merck. Cyclohexane, dichloromethane, heptane, pentane, toluene, methanol and anhydrous diethyl ether (spectroscopic grade, Aldrich Chemical) were used as received. *p*-Xylene (Aldrich Chemical) was distilled over CaF_2 from mixed xylenes, and used immediately. THF (Flucka) was distilled over sodium metal and benzophenone and used immediately. Argon and carbon monoxide were supplied by Air Products.

4.2. Equipment

Infrared spectra were recorded on a Perkin–Elmer 2000 FT-IR spectrometer using sodium chloride windows (d = 0.1 mm), and spectroscopic grade cyclohexane, pentane or chloroform. NMR (^1H and ^{13}C) spectra were measured on a Bruker model AC400 MHz spectrometer in appropriate deuterated solvents at room temperature. The peaks were calibrated according to the internal tetramethylsilane (TMS) standard. UV–Vis spectra were recorded on a Hewlett–Packard 8452A photodiode array spectrometer, using quartz cells of 1 cm path length. In the steady-state photolysis, wavelength selection was achieved using Corning cut-off filters.

The excitation source in the flash photolysis experiments was a pulsed neodymium yttrium aluminium garnet (Nd-YAG) laser from Spectron Laser Systems, operating at 1064 nm. The frequency of 1064 nm may be doubled, tripled, or quadrupled to generate a second, third or fourth harmonic frequency of 532 nm, 355 nm, or 266 nm, respectively, as required. The power of the laser may be amplified by applying different voltages across the amplifier flash tube. The duration of the laser pulse is in the region of 10 ns. The apparatus has been described in detail elsewhere [7].

All samples for laser flash photolysis experiments were prepared in a sealable degassing bulb attached to a fluorescence cell. Samples are prepared by dissolution in the appropriate spectroscopic grade solvent, such that the absorbance at λ_{exc} (532, 355, or 266 nm) was between 0.6 and 1.0 AU. The sample was degassed by three cycles of the freeze–pump–thaw procedure to a pressure of 10^{-2} Torr. Subsequently, the sample is liquid pumped to remove any trace amounts of water that may be present [12], before the appropriate atmosphere (CO or Ar) was admitted to the cell.

The matrix isolation apparatus consists of a closed cycle helium refrigerator, sample window, shroud, deposition tube, gas mixing chamber, gas inlet, backing pump, diffusion pump and temperature control unit. Matrixes were deposited onto a CaF_2 window cooled to 20 K, with matching outer windows on the vacuum shroud. Samples for infrared spectroscopy and for UV–Vis spectra were deposited onto a CaF_2 window cooled by a CS202 closed-cycle refrigerator to 20 K. A thermocouple embedded in a cavity beside the window and connected to the temperature control unit which maintained the temperature by varying the current through heating elements next to the sample. The system pumps to 8×10^{-4} mbar prior to cooling and achieves 10^{-7} mbar upon cooling to 20 K. Host gases (Cryo Service) are deposited onto a window via a needle valve A ratio of sample molecule to host matrix in the region 1:2000 is desirable. Typically the rate of gas deposition of 0.6 Torr/min. achieves sufficient dilution on the matrix window. Both the sample and gas are deposited simultaneously. (η^3-allyl)$Fe(CO)_2NO$ was sublimed from a right angled tube at 22 °C as the gas stream entered the vacuum shroud. The sample was deposited onto the windows at 20 K, and monitored in the infrared until the absorbance of one of the metal carbonyl bands was approximately 1 AU. When the required absorbance was achieved the samples were photolysed and monitored on a Spectrum One FTIR spectrophotometer. Spectra were recorded at 1 cm^{-1} resolution with eight scans. UV–Vis spectra were recorded on a Perkin–Elmer Lambda spectrophotometer. Matrixes were photolysed through a quartz window with a 300 W Xe arc in combination with a water filter to remove the IR component. Photolysis wavelengths were selected with cut-off filters: λ_{exc} >500, >410 or 310 nm.

4.3. Synthesis of (η^3-C_3H_5)$Fe(CO)_2(NO)$

The synthesis of (η^3-C_3H_5)$Fe(CO)_2(NO)$ was achieved by the method of Pauson and co-workers [13]. This method involves firstly synthesising the precursor complex, $[Fe(CO)_2NO]^-Na^+$. The synthesis of $[Fe(CO)_2NO]^-Na^+$ used the method of Hieber and Beuttner [14], which involves treating $Fe(CO)_5$ (2.5 cm^3, 18.6 mmol) with equimolar $NaNO_2$ in the presence of sodium metal (1 g) in absolute methanol (100 ml). The mixture was heated to its reflux temperature for 1 h in the dark under an argon atmosphere. The filtrate was removed and dissolved in

anhydrous diethylether (40 cm^3), to which 20 cm^3 of *p*-xylene was then added. The solution was then concentrated under reduced pressure until a precipitate of the desired $[Fe(CO)_3NO]^-Na^+$ had formed. The product was then collected by filtration under argon, with yields (based on $NaNO_2$), in the range 80–90%.

Allyl bromide (0.7 cm^3, 7.7 mmol) was dissolved in 10 cm^3 of anhydrous diethylether. This solution was added to $[Fe(CO)_3NO]^-Na^+$ (1.5 g, 7.7 mmol) dissolved in 50 cm^3 of diethylether. The solution was heated to 40 °C for 24 h during which time the colour changed from orange to red. The solution was then filtered and the solvent removed under reduced pressure yielding a red oil. The dark red product was isolated by chromatography on neutral alumina using pentane as the mobile phase. Typical yields for the oil, based on allyl bromide, were in the 70–80% range.

Spectroscopic data: IR (C_6H_{12}): ν_{CO} 2035, 1980 cm^{-1}; ν_{NO} 1756 cm^{-1}; ^1H NMR ($CDCl_3$, δ/ppm): 3.12 (d, 2H), 3.95 (d, 2H), 4.3 (m, 1H).

4.4. Synthesis of (η^3-2-chloroallyl)Fe(CO)$_2$NO

The synthesis of (2-η^3-C_3H_4Cl)$Fe(CO)_2NO$ was carried out according to the method of Cardaci with some minor modifications [10]. Typically equimolar amounts of 2,3-dichloropropene (0.9 ml, 12 mmol) dissolved in anhydrous diethyl ether (10 ml) and $[Fe(CO)_3NO]^-Na^+$ (1.5 g, 7.7 mmol) were allowed to react in diethyl ether (50 ml). Reaction progress was monitored using IR spectroscopy. The mixture was heated to its reflux temperature for 24 h. Subsequently, the mixture was filtered, and the solvent removed under reduced pressure, yielding a dark red oil. The oil was chromatographed on alumina. Elution with pentane yielded a deep red oil. Typical yield was in the range 65–70%. Spectroscopic data: IR (C_6H_{12}): ν_{CO} 2045, 1993 cm^{-1}; ν_{NO} 1760 cm^{-1}; ^1H NMR ($CDCl_3$, δ/ppm): 3.80 (s, 2H), 4.36 (s, 2H).

4.5. Synthesis of (η^3-C_3H_5)Fe(CO)(NO)(PPh_3)

For the synthesis of (η^3-C_3H_5)Fe(CO)(NO)(PPh_3) the method used by Pauson and co-workers was modified slightly [13]. Triphenylphosphine (1.5 g, 6 mmol) was added to a solution of (η^3-C_3H_5)$Fe(CO)_2(NO)$ (1.1 g, 6 mmol) in cyclohexane (50 cm^3). The solution was brought to its reflux temperature for 48 h under an argon atmosphere. The resulting solution was then filtered and the solvent removed under reduced pressure. The product was isolated by chromatography on silica, (η^3-C_3H_5)Fe-$(CO)_2(NO)$ was eluted using pentane, while a mixture of dichloromethane and pentane (1:4) eluted (η^3-C_3H_5)Fe-(CO)(NO)(PPh_3) as a red solid. Yields were typically in the range 50–60% based on the (η^3-C_3H_5)$Fe(CO)_2(NO)$ starting material.

Spectroscopic data: IR (C_6H_{12}): ν_{CO} 1945 cm^{-1}; ν_{NO} 1710 cm^{-1}; ^1H NMR ($CDCl_3$, δ/ppm): 2.80 (d, 2H), 3.59 (d, 2H), 5.2 (m, 1H), 7.39 (m, 15H).

4.6. Synthesis of (η^3-C_3H_5)Fe(NO)(PPh_3)$_2$

Triphenylphosphine (3.0 g, 12 mmol) was added to a solution of (η^3-C_3H_5)Fe(CO)(NO)(PPh_3) in *n*-heptane (50 cm^3). The solution was then heated to its reflux temperature for 5 days under an argon atmosphere. Upon cooling, the solvent was removed under reduced pressure, and the resulting crude solid was washed repeatedly until free of PPh_3 and (η^3-C_3H_5)Fe(CO)(NO)(PPh_3). The remaining red solid was characterised by IR and ^1H NMR spectroscopy (Table 1). Yields were low, usually below 5% based on (η^3-C_3H_5)Fe(CO)(NO)(PPh_3).

Spectroscopic data: IR ($CHCl_3$): ν_{NO} 1669 cm^{-1}; ^1H NMR ($CDCl_3$, δ/ppm): 2.74 (s, 2H), 3.58 (s, 2H), 4.15 (m, 1H), 7.41 (m, 12H), 7.48 (d, 6H), 7.60 (q, 12H).

Acknowledgements

The authors thank Enterprise Ireland and Dublin Corporation for financial assistance.

References

[1] K. Szaciłowski, A. Chmura, Z. Stasicka, Coord. Chem. Rev. 249 (21) (2005) 2408, and references therein.
[2] (a) P.C. Ford, S. Wecksler, Coord. Chem. Rev. 249 (13) (2005) 1382; (b) E. Tfouni, M. Krieger, B.R. McGarvey, D.W. Franco, Coord. Chem. Rev. 236 (1) (2003) 57.
[3] P. Crichton, M. Poliakoff, A.J. Rest, J.J. Turner, J. Chem. Soc., Dalton Trans. (1973) 1321.
[4] W. Wang, F. Chen, J. Lin, Y. She, J. Chem. Soc., Faraday Trans. 91 (1995) 847.
[5] E.G. Moore, Q.H. Gibson, J. Biol. Chem. 251 (1976) 2788; E.J. Rose, B.M. Hoffman, J. Am. Chem. Soc. 105 (1983) (1983) 2866.
[6] J. Bourassa, P.C. Ford, Coord. Chem. Rev. 200 (2000) 887.
[7] J. Bourassa, W. DeGraff, S. Kudo, D.A. Wink, J.B. Mitchell, P.C. Ford, J. Am. Chem. Soc. 119 (1997) 2853.
[8] B.S. Creaven, M.W. George, A.G. Ginzburg, C. Hughes, J.M. Kelly, C. Long, I.M. McGrath, M.T. Pryce, Organometallics 12 (1993) 3127.
[9] B.S. Creaven, A.J. Dixon, J.M. Kelly, C. Long, M. Poliakoff, Organometallics 6 (1987) 2600.
[10] G. Cardaci, A. Foffani, J. Chem. Soc., Dalton Trans. (1974) 1808.
[11] S.P. Church, F.-W. Grevels, H. Hermann, J.M. Kelly, W.E. Klotzbücher, K. Schaffner, J. Chem. Soc., Chem. Commun. (1985) 594.
[12] C.J. Breheny, J.M. Kelly, C. Long, S. O'Keeffe, M.T. Pryce, G. Russell, M. Walsh, Organometallics 17 (1998) 3690.
[13] F.M. Chaudhari, G.R. Knox, P.L. Pauson, J. Chem. Soc. (C) (1967) 2255.
[14] W. Hieber, H. Beuttner, Z. Naturforsch. B 15 (1960) 101.